

Distilling Optimal Neural Networks: Rapid Search in Diverse Spaces

Bert Moons¹, Parham Noorzad², Andrii Skliar¹, Giovanni Mariani¹,
Dushyant Mehta¹, Chris Lott² and Tijmen Blankevoort¹
Qualcomm AI Research*

¹Qualcomm Technologies Netherlands B.V.

²Qualcomm Technologies, Inc

{bmoons, parham, askliar, gmariani, dmehta, clott, tijmen}@qti.qualcomm.com

Abstract

This work presents DONNA (Distilling Optimal Neural Network Architectures), a novel pipeline for rapid neural architecture search and search space exploration, targeting multiple different hardware platforms and user scenarios. In DONNA, a search consists of three phases. First, an accuracy predictor is built for a diverse search space using blockwise knowledge distillation. This predictor enables searching across diverse macro-architectural network parameters such as layer types, attention mechanisms, and channel widths, as well as across micro-architectural parameters such as block repeats, kernel sizes, and expansion rates. Second, a rapid evolutionary search phase finds a Pareto-optimal set of architectures in terms of accuracy and latency for any scenario using the predictor and on-device measurements. Third, Pareto-optimal models can be quickly finetuned to full accuracy. With this approach, DONNA finds architectures that outperform the state of the art. In ImageNet classification, architectures found by DONNA are 20% faster than EfficientNet-B0 and MobileNetV2 on a Nvidia V100 GPU at similar accuracy and 10% faster with 0.5% higher accuracy than MobileNetV2-1.4x on a Samsung S20 smartphone. In addition to neural architecture search, DONNA is used for search-space exploration and hardware-aware model compression.

1. Introduction

Although convolutional neural networks (CNN) are state-of-the-art on several vision tasks, they do not always execute efficiently on hardware platforms. To alleviate this issue, CNNs are specifically optimized to minimize latency and energy consumption for on-device performance. However, the architecture of an optimal CNN architecture can

vary significantly between different platforms. Even on a given hardware platform, their efficiency can change with different operating conditions or driver versions. To solve this problem, low-cost methods for automated hardware-aware neural architecture search (NAS) are required.

Current NAS algorithms, however, suffer from several limitations. First, many optimization algorithms [28, 11, 27, 18] target only a single *deployment scenario*, be it a hardware-agnostic complexity metric, a hardware platform, or different latency, energy, or accuracy requirements. This means their full search effort has to be repeated whenever any part of that scenario changes. Second, there are no methods that can search through truly diverse search spaces of potential architectures with limited resources. Current methods either search through large and diverse spaces at a prohibitively expensive search cost [28, 11], or limit their scope and applicability by trading search time for a more constrained and less diverse search [3, 27, 29, 37, 20]. Most of such speedups in NAS come from a heavy reliance on weight sharing mechanisms, which require all architectures in the search space to be structurally similar. Thus, these works can only search among *micro-architectural* choices such as kernel sizes, expansion rates, and block repeats and not among general *macro-architectural* choices of layer types, attention mechanisms, channel widths, and activation functions. For an optimal macro-architecture in terms of layers, attention, and activation, these works rely on prior searches using expensive diverse methods such as [28, 11].

This work introduces DONNA (Distilling Optimal Neural Network Architectures), a method that addresses both issues: it scales up graciously towards multiple deployment scenarios and performs rapid NAS in diverse search spaces. The first issue is resolved by splitting NAS into a scenario-agnostic training phase and a scenario-aware search phase that requires only limited training, as in Figure 1. After an accuracy predictor is built in the training phase, the search is executed quickly for each new deployment scenario, typically in the time-frame of hours and only requir-

*Qualcomm AI Research is an initiative of Qualcomm Technologies, Inc.

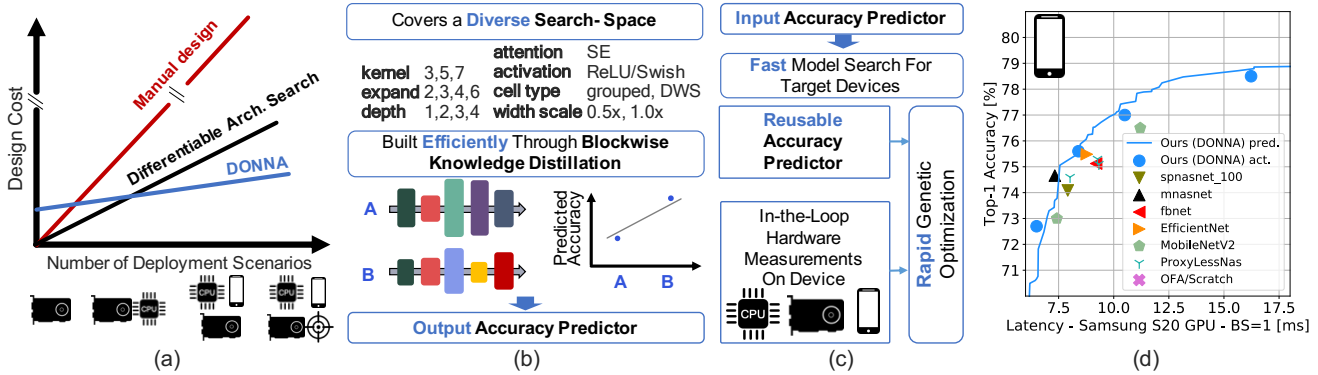


Figure 1: Neural networks are deployed in many scenarios, on various hardware platforms with varying power modes and driver software, or with different speed and accuracy requirements. DONNA scales gracefully towards NAS for a large amount of scenarios, contrary to prior approaches where NAS is repeated for each of them (a). This is achieved by splitting NAS into a scenario-agnostic training phase building an accuracy predictor using blockwise knowledge distillation (b) and a rapid scenario-aware search phase using this predictor and hardware measurements (c). This yields a state-of-the-art Pareto-front of architectures on-device, illustrated here for a Samsung S20 GPU classifying ImageNet [8] images (d).

ing minimal fine-tuning to finalize optimal models. Second DONNA considers diverse *macro-architectural* choices in addition to *micro-architectural* choices, by creating an accuracy predictor through Blockwise Knowledge Distillation (BKD) [16], see Figure 3. This approach imposes little constraints on the macro and micro-architectures under consideration, allowing a vast, diverse, and extensible search space. The DONNA pipeline yields state of the art network architectures, as illustrated for a Samsung S20 GPU in Figure 1(d). Finally, we use DONNA for rapid search space exploration and on-device model compression. This is possible as the DONNA accuracy predictor generalizes to architectures outside of the original search space. The main contributions of this work are the following:

- We introduce DONNA, a novel three-step pipeline for scenario-aware NAS supporting rapid search in diverse spaces with varying macro- and micro-architectures.
- We evaluate the effectiveness of DONNA, both on ImageNet [8] and MS-COCO [17] for different hardware-agnostic and hardware-aware targets.
- We show the DONNA accuracy predictor generalizes to unseen search spaces. This is useful for fast search-space exploration by reusing previously built predictors on a different search space.
- We demonstrate the use of DONNA for compressing pre-trained models with different arbitrary layer types, for on-device acceleration.

2. Related Work

Over time NAS literature has evolved from prohibitively expensive, but holistic and diverse search methods [38, 39, 28] to lower cost approaches that search in more constrained non-diverse search spaces [3, 27]. This work, DONNA, allows the best of both worlds: rapid search in diverse spaces.

Early approaches to NAS rely on reinforcement learning [38, 39, 28] or evolutionary optimization [25]. These methods allow for diverse search spaces, but at infeasibly high search times, training thousands of full models for a number of epochs throughout the search. MNasNet [28] for example, uses up to 40,000 epochs in a single search. The search can be sped up by using weight sharing among different models, as in ENAS [23]. However, this comes at the cost of a less diverse search space, as the subsampled models have to be similar for the weights to be shareable.

In another line of work, differentiable architecture search methods such as DARTS [18], FBNet [34], FBNetV2 [31], ProxylessNAS [4], AtomNAS [21] and Single-Path NAS [27] simultaneously optimize the weights of a large supernet and its architectural parameters. This poses several impediments to scalable and scenario-aware NAS in diverse search spaces. First, in most of these works, different cell choices have to be available to the algorithm, ultimately limiting the space’s size and diversity. While several works attempt to address this problem either by trading off the number of architecture parameters against the number of weights that are in GPU memory at a given time [5], by updating only a subset of the weights during the search [36], or by exploiting more granular forms of weight-sharing [27], the fundamental problem remains whenever new operations are introduced. Second, although differ-

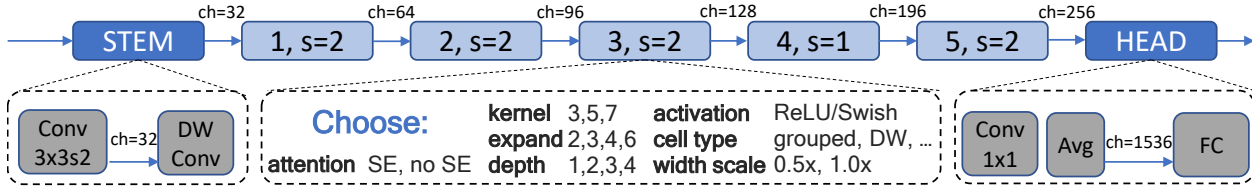


Figure 2: DONNA splits a model in a stem, head and N blocks. The search space is defined over the N blocks with varying kernel size, expand, depth, activation, cell type, attention and width scale factors. Block strides are kept constant.

entiable search methods speed up a single search iteration, the search must be repeated for every scenario due to their coupling of accuracy and complexity. Differentiable methods also require differentiable cost models. Typically these models use the sum of layer latencies as a proxy for the network latency, which can be inaccurate. This is especially the case in emerging depth-first processors [10], where intermediate results are stored in the local memory, making full-graph latency depend on layer sequences rather than on individual layers.

To improve the scaling performance of NAS across different scenarios, it is critical to decouple the accuracy prediction of a model from the complexity objective. In Once-for-All (OFA) [3], a large weight-sharing supernet is trained using progressive shrinking. This process allows the sampling of smaller subnets from the trained supernet that perform comparably with models that have been trained from scratch. A large number of networks can then be sampled to build an accuracy predictor for this search space, which in turn can be used in a scenario-aware evolutionary search, as in Figure 1(c). Although similar to DONNA in this approach, OFA [3] suffers from several disadvantages. First, its search space’s diversity is limited due to its reliance on progressive shrinking and weight sharing, which requires a fixed macro-architecture in terms of layer types, attention, activations, and channel widths. Furthermore, progressive shrinking can only be parallelized in the batch dimension, limiting the maximum number of GPUs that can process in parallel. DONNA does not suffer from these constraints.

Similarly, Blockwisely-Supervised NAS (DNA) [16], splits NAS into two phases: the creation of a ranking model for a search space and a custom targeted search to find the highest-ranked models at a given constraint. To build this ranking model, DNA uses blockwise knowledge distillation (BKD) to build a relative ranking of all possible networks in a given search space. This network should then be trained from scratch and verified. It is crucial to note that it is BKD that enables the diverse search for optimal attention mechanisms, activation functions, and channel scaling. However, the DNA method has three disadvantages: (1) the simplistic ranking model fails when ranking large and diverse search spaces (Section 3.2), (2) the ranking only holds within a given search space and does not allow the comparison of

different search spaces easily and (3) because of the reliance on training subsampled architectures from scratch, the method is not competitive in terms of search time. The method proposed in this work, DONNA, addresses all these issues. We refer the reader to [9] for a more comprehensive overview of the NAS-literature.

3. Distilling Optimal Neural Networks

DONNA is a three step pipeline for NAS. For a given search space (Section 3.1), we first build a deployment-scenario-agnostic accuracy predictor once using Blockwise Knowledge Distillation (BKD) (Section 3.2). Second, a rapid scenario-aware evolutionary search phase finds the Pareto-optimal network architectures for any specific scenario (Section 3.3). Third, the predicted Pareto-optimal architectures can be quickly finetuned up to full accuracy for deployment (Section 3.4).

3.1. Search Space Structure

Figure 2 illustrates the block-level architecture of our search spaces and some parameters that can be varied within it. This search space is comprised of a stem, head, and N variable blocks, each with a fixed stride. The choice of stem, head and the stride pattern depends on the choice of the reference model. The blocks used here are comprised of repeated layers, linked together by feedforward and residual connections. Throughout the text and in Appendix A, other reference models based on MobileNetV3 [11], ProxyLess-NAS [4] and EfficientNet [29] are discussed.

The blocks in the search space are denoted $B_{n,m}$, where $B_{n,m}$ is the m^{th} potential replacement out of M choices for block B_n in the reference model. These blocks can be of any style of neural architecture, with very few structural limitations; only the spatial dimensions of the input and output tensors of $B_{n,m}$ need to match those of the reference model. This flexibility allows DONNA to search macro-architectural parameters in a diverse search-space.

3.2. Blockwise Accuracy Prediction

3.2.1 Blockwise Knowledge Distillation

We discuss Blockwise Knowledge Distillation (BKD) as the first step in building an accuracy predictor for our search

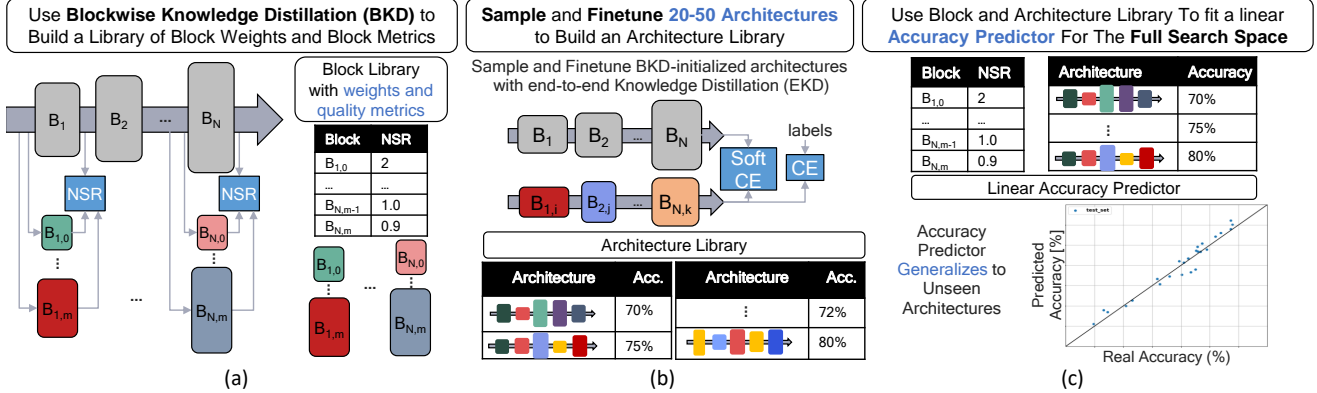


Figure 3: An accuracy predictor is built in three steps. (a) Blockwise knowledge distillation (BKD) is executed to build a library of block-quality metrics and pretrained weights. (b) A set of full-model architectures is sampled from the search space and finetuned using the BKD initialization. (c) These results are used as targets to fit a linear accuracy predictor.

space, see Figure 3(a). BKD yields a *Block Library* of pretrained weights and quality metrics for each of the replacement blocks $B_{n,m}$. This is later used for fast finetuning (Section 3.4) and to fit the accuracy predictor (Section 3.2.2). To build this library, each block $B_{n,m}$ is trained independently as a student using the pretrained reference block B_n as a teacher. The errors between the teacher’s output feature map Y_n and the student’s output feature map $\bar{Y}_{n,m}$ are used in this process. Formally, this is done by minimizing the per-channel noise-to-signal-power ratio (NSR):

$$\mathcal{L}(W_{n,m}; Y_{n-1}, Y_n) = \frac{1}{C} \sum_{c=0}^C \frac{\|Y_{n,c} - \bar{Y}_{n,m,c}\|^2}{\sigma_{n,c}^2} \quad (1)$$

Here C is the number of channels in a feature map, $W_{n,m}$ are the weights of block $B_{n,m}$, Y_n is the target output feature map of B_n , $\bar{Y}_{n,m}$ is the output of block $B_{n,m}$ and $\sigma_{n,c}^2$ is the variance of $Y_{n,c}$. This metric is closely related to Mean-Square-Error (MSE) on the feature maps, which [22] shows to be correlated to the task loss.

Essentially, the blocks $B_{n,m}$ are trained to replicate the teacher’s non-linear function $Y_n = B_n(Y_{n-1})$ as closely as possible. Intuitively, larger, more accurate blocks with a larger “modeling capacity” replicate this function more closely than smaller, less accurate blocks. On ImageNet such knowledge distillation requires only a *single* epoch of training for effective results. After training each block, the resulting NSR metric is added to the Block library as a *quality metric* of the block $B_{n,m}$. Note that the total number of blocks $B_{n,m}$ grows linearly as $N \times M$, whereas the overall search space grows exponentially as M^N , making the method scale well even for large search-spaces.

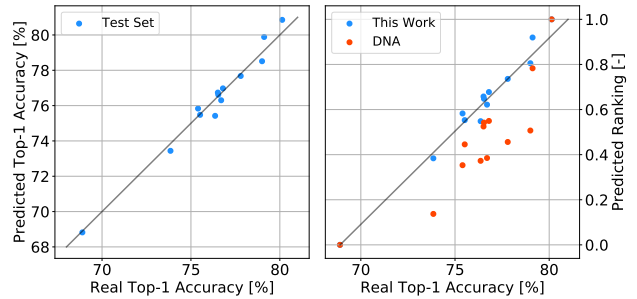


Figure 4: The linear accuracy predictor generalizes to a test-set of unseen models (left), and is a better ranking predictor than DNA [16] (right) on the same set: Kendall-Tau [14] of 0.9 in this work versus 0.78 for DNA.

3.2.2 Linear Accuracy Predictor

The key insight behind DONNA is that block-level quality metrics derived through BKD (e.g., per-block NSR) can be used to predict the accuracy of all architectures sampled from the search space. We later show this metric even works for architectures outside of the search space (Section 4.1.2).

To create an accuracy predictor, we build an *Architecture Library* of trained models sampled from the search space, see Figure 3(b). These models can be trained from scratch or finetuned quickly using weight initialization from BKD (Section 3.4). Subsequently, we fit a linear regression model, typically using second-order terms, to predict the full search space’s accuracy using the quality metrics stored in the Block Library as features and the accuracy from the Architecture Library as targets. Figure 4(left) shows that linear predictor fits well with a test-set of network architectures trained on ImageNet [8] in the DONNA space. This predictor can be understood as a sensitivity model that indicates which blocks should be large, and which ones

can be small, to build networks with high accuracy. Appendix A.4.2 discusses the effectiveness of different derived quality metrics on the quality of the accuracy prediction.

This process is now compared to DNA [16], where BKD is used to build a ranking-model rather than an accuracy model. DNA [16] ranks subsampled architectures i as:

$$R_i = \sum_{n=0}^N \frac{\|Y_n - \bar{Y}_{n,m_i}\|_1}{\sigma_n} \quad (2)$$

which is sub-optimal due to two reasons. First, a ranking model only ranks models within the same search space and does not allow comparing performance of different search spaces. Second, the simple sum of quality metrics does not take the potentially different noise-sensitivity of blocks 1 to N into account, for which a weighted sensitivity model is required. The DONNA predictor takes both roles. Figure 4(right) illustrates the performance of the linear predictor for the DONNA search space and compares the quality of its ranking to DNA [16]. Note that the quality of the DONNA accuracy predictor increases over time, as whenever searched Pareto-optimal networks are trained or finetuned, they can be added to the Architecture Library, and the predictor can be fitted again.

3.3. Evolutionary Search

Given the accuracy model and the block library, the NSGA-II [7, 1] evolutionary algorithm is executed to find Pareto-optimal architectures that maximize model accuracy and minimize a target cost function, see Figure 1(c). The cost function can be scenario-agnostic, such as the number of operations or the number of parameters in the network, or scenario-aware, such as on-device latency, throughput, or energy. In this work, full-network latency is considered as a cost function by using direct hardware measurements in the optimization process. At the end of the optimization process, the Pareto-optimal models yielded by the NSGA-II are finetuned to obtain the final models (Section 3.4).

3.4. Finetuning Architectures

Full architectures sampled from the search space can be quickly finetuned to match the from-scratch training accuracy by initializing them with weights from the BKD process (Section 3.2.1). Finetuning is further sped up by using end-to-end knowledge distillation (EKD) using the reference model as a teacher, see Figure 3(b). In Appendix A.5, we show such models can be finetuned up to state-of-the-art accuracy in 15-50 epochs depending on the reference model and the complexity and diversity of the search space. This is a 9 – 30× speedup compared to the state-of-the-art 450 epochs required in [33] for training EfficientNet-style networks from scratch. This rapid training scheme is crucial to the overall efficiency of DONNA, since we use it for both,

generating training targets for the linear accuracy predictor in Section 3.2, as well as to quickly finetune and verify Pareto-optimal architectures.

4. Experiments

This section discusses three use-cases of DONNA: scenario-aware neural architecture search (Section 4.1.1), search-space extrapolation and design (Section 4.1.2), and model compression (Section 4.1.3). Additionally, we show that architectures found by DONNA transfer to optimal backbones for EfficientDet-style [30] object detection on MS-COCO [17] (Section 4.2).

4.1. ImageNet Classification

We present experiments for five different search spaces for ImageNet classification: DONNA, EfficientNet-Compression, MobileNetV3 (1.0×, 1.2×) and ProxylessNas (1.3×). The latter three search spaces are *blockwise* versions of the spaces considered by OFA [2]; that is, parameters such as expansion ratio and kernel size are modified on the block level rather than at the layer level. Results for the DONNA and EfficientNet space are discussed in this section, other results can be found in Appendix A.6. We show that networks found by DONNA outperform the state-of-the-art. For example, DONNA is up to 2.4% more accurate on ImageNet [8] validation compared to OFA[3] trained from scratch with the same amount of parameters. At the same time, DONNA finds models outperforming DNA [16] up to 1.5% on a V100 GPU at the same latency and MobileNetV2 (1.4×) by 10% at 0.5% higher accuracy on the Samsung S20 GPU, see Figure 5. All experiments are for ImageNet [8] images using 224 × 224 input resolution. Training hyperparameters are discussed in Appendix A.1.

4.1.1 NAS for DONNA on ImageNet

DONNA is used for *scenario-aware Neural Architecture Search* on ImageNet [8], quickly finding state-of-the-art models for a variety of deployment scenarios, see Figure 5.

As shown in Figure 2, all 5 blocks B_n in the DONNA space can be replaced by a choice out of $M = 384$ options: $k \in \{3,5,7\}$; $\text{expand} \in \{2,3,4,6\}$; $\text{depth} \in \{1,2,3,4\}$; $\text{activation} \in \{\text{ReLU}, \text{Swish}[11]\}$; $\text{attention} \in \{\text{None}, \text{SE}[12]\}$; $\text{layer-type} \in \{\text{grouped}, \text{depthwise inverted residual bottleneck}\}$; and $\text{channel-scaling} \in \{0.5\times, 1.0\times\}$. The search-space can be expanded or arbitrarily constrained to known efficient architectures for a device. Each of these $5 \times 384 = 1920$ alternative blocks is trained using BKD to complete the Block Library. Once the Block Library is trained, we use the BKD-based ranking metric from DNA[16] to sample a set of architectures uniformly spread over the ranking space. For the DONNA search space, we finally finetune the sampled networks for 50

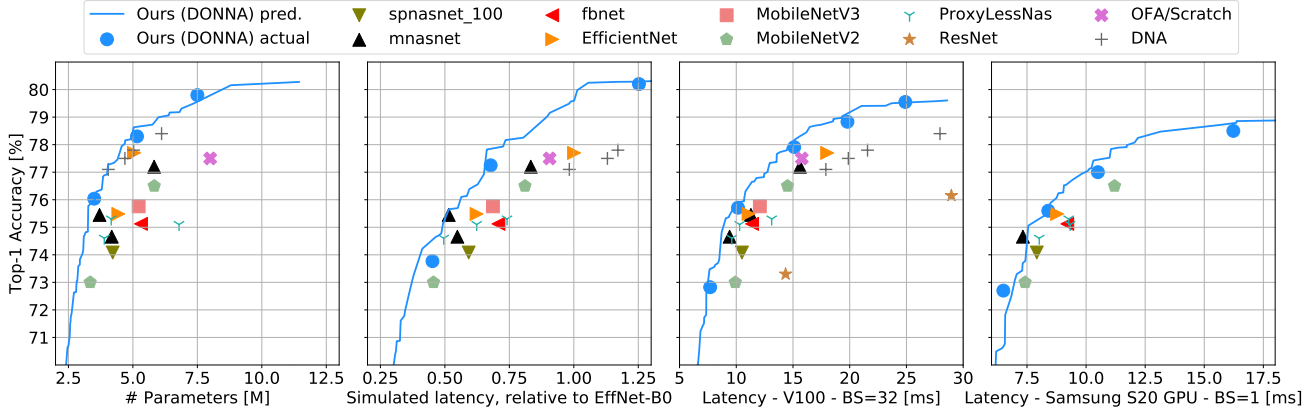


Figure 5: The predicted Pareto-optimal front and models found by DONNA, when optimizing for the number of parameters (left), and latency on a simulator targeting tensor compute units in a mobile SoC (mid left), an Nvidia V100 GPU (mid right) and a Samsung S20 (right). The trend line indicates predicted accuracy, whereas the dots are sampled from the predicted trend line and finetuned up to the level of from-scratch accuracy.

Table 1: Comparing the cost of NAS methods, assuming 10 trained architectures per deployment scenario. DONNA can search in a diverse space similar to MNasNet [28] at a $100\times$ lower search-cost.

| Method | Granularity | Macro-Diversity | Search-cost 1 scenario [epochs] | Cost / Scenario 4 scenarios [epochs] | Cost / Scenario ∞ scenarios [epochs] |
|--------------|-------------|-----------------|------------------------------------|---|--|
| OFA [3] | layer-level | fixed | $1200+10\times[25-75]$ | 550 – 1050 | 250 – 750 |
| DNA [16] | layer-level | fixed | $770+10\times 450$ | 4700 | 4500 |
| MNasNet [28] | block-level | variable | $40000+10\times 450$ | 44500 | 44500 |
| This work | block-level | variable | $4000 + 10\times 50$ | 1500 | 500 |

epochs starting from the BKD initialization, building an Architecture Library with accuracy targets used to fit the linear accuracy predictor. Typically, 20-30 target networks need to be finetuned to yield good results, see Appendix A.4.

In total, including the training of a reference model (450 epochs), $450 + 1920 + 30 \times 50 = 3870$ epochs of training are required to build the accuracy predictor. This is less than $10\times$ the cost of training a single network from scratch to model the accuracy of more than 8 trillion architectures. Subsequently, any architecture can be selected and trained to full accuracy in 50 epochs, starting from the BKD initialization. Similarly, as further discussed in Appendix A.4, an accuracy model for ProxylessNAS ($1.3\times$), MobileNetV3 ($1.2\times$), EfficientNet-Compressed costs $450 + 135 + 20 \times 50 = 1585$ epochs, roughly the same as training 4 models from scratch. Although this is a higher cost than OFA [3], it covers a much more diverse search space. OFA requires an equivalent, accounting for dynamic batch sizes [2], of $180 + 125 + 2 \times 150 + 4 \times 150 = 1205$ epochs of progressive shrinking with backpropagation on a large supernet. BKDNAS [16] requires only $450 + 16 \times 20 = 770$ epochs to build its ranking model, but 450 epochs to train models from scratch. Other methods like MNasNet [28] can handle a similar diversity as DONNA, but typically require an

order of magnitude longer search time (40000 epochs) *for every deployment scenario*. DONNA offers MNasNet-level diversity at a 2 orders of magnitude lower search cost. On top of that, BKD epochs are significantly faster than epochs on a full network, as BKD requires only partial computation of the reference model and backpropagation on a single block $B_{n,m}$. Moreover, and in contrast to OFA, all blocks $B_{n,m}$ can be trained in parallel since they are completely independent of each other. Table 1 quantifies the differences in search-time between these approaches.

With the accuracy predictor in place, Pareto-optimal DONNA models are found for several targets and deployment scenarios. Figure 5 shows DONNA finds networks that outperform the state of the art in terms of the number of parameters, latency on a simulator targeting tensor compute units in a mobile SoC, an NVIDIA V100 GPU, and on the GPU of a Samsung S20 phone. The figure shows the predicted Pareto-front resulting from the evolutionary search, and the actual finetuned models selected from the predicted Pareto fronts. Every predicted Pareto-optimal front is generated using an evolutionary search with NSGA-II [7, 1] on a population of 100 architectures until convergence. Where applicable, full-architecture latency measurements on hardware are used in the evolutionary loop. Details on measure-

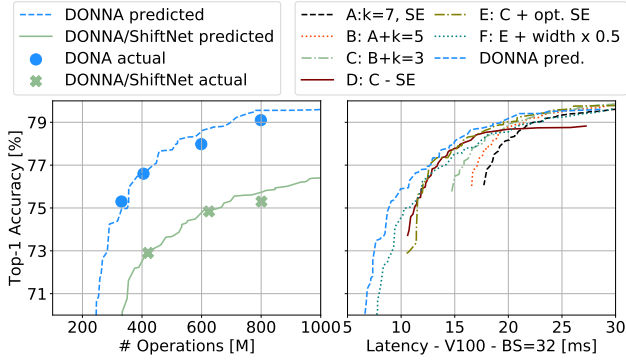


Figure 6: An accuracy predictor for DONNA generalizes to a space with ShiftNets [35], without using ShiftNets to train the predictor (left). Predicted performance of variations on the DONNA search space on a V100 GPU (right). A baseline (A) considers SE and swish in every block and $k \in \{7\}$, $\text{expand} \in \{3,4,6\}$ and $\text{depth} \in \{2,3,4\}$. Other lines show results for search spaces built starting from (A), e.g. (B) considers $k \in \{5,7\}$, and (C) $k \in \{3,5,7\}$, and so on.

Table 2: DONNA finds similar models to MobileNetV3 [11] in the MobileNetV3 (1.0 \times) space.

| Network | Number of Operations [M] | ImageNet val top-1 [%] |
|-------------------------------|--------------------------|------------------------|
| MobileNetV3 [11] | 232 | 75.77@600[33] |
| Ours (MobNetV3 1.0 \times) | 242 | 75.75@50 |

ments and baseline accuracy are given in Appendix A.3.

Similarly, Table 2 shows that DONNA finds models in the MobileNetV3 (1.0 \times) space that are on par with MobileNetV3 [11] in terms of number of operations, although [11] is found using expensive MNasNet [28]. More results for other search spaces are shown in Figure 10 in Appendix A.6. We also visualize Pareto-optimal DONNA models for different platforms in Appendix C.

4.1.2 Search-Space Design, Exploration and Extension

The DONNA approach can also be used for *rapid search space design and exploration*. Using DONNA, a designer can quickly determine whether the search space should be extended or constrained for optimal performance.

Such extension is possible because the DONNA accuracy predictor generalizes to previously unseen architectures, without having to extend the Architecture Library. Figure 6(left) shows this extrapolation works when extending to blocks based on ShiftNets [35]. Note how the trend-line predicts the performance of full Pareto optimal ShiftNets even though the predictor is created without any ShiftNet data. Here, ShiftNets are our implementation, with learned shifts per group of 32 channels depthwise-separable

replacement. These generalization capabilities are obtained because the predictor only uses BKD quality metrics as an input without requiring any structural information about the replacement block. This feature is a major advantage of DONNA compared to OFA [3] where the predictor cannot generalize to completely different layer-types.

This quick prototyping capability is also showcased for the DONNA search space on a V100 GPU in Figure 6(right). We use the same methodology as before for design space exploration [24] and verify potential gains in expanding the search space. For good performance on GPU, it is crucial to have diverse macro-architectural choices, such as searching over Squeeze-and-Excite (SE [12]) per block. The full DONNA space finds networks that are 30% faster than a similar space with fewer choices in expansion ratios and with Squeeze-and-Excite in every block. Every plotted line in Figure 6 (right) is a predicted Pareto-optimal front for a variation of the search space. A baseline (A) considers SE and swish in every block and $k \in \{7\}$, $\text{expand} \in \{3,4,6\}$ and $\text{depth} \in \{2,3,4\}$. Other lines show results for search spaces built starting from (A), e.g. (B) considers $k \in \{5,7\}$, (C) $k \in \{3,5,7\}$, (D) removes SE and swish, (E) allows choosing optimal placement of SE and Swish, (F) adds a channel-width multiplier and full DONNA adds $\text{expand} \in \{2,3,4,6\}$ and $\text{depth} \in \{1,2,3,4\}$. This approach quickly shows the impact of choices in the search space on real hardware, without requiring a novel predictor.

4.1.3 Model Compression

DONNA is also used for *hardware-aware compression of existing neural architectures* into faster, more efficient versions. This is useful for a designer who has prototyped a network for their application and wants to run it efficiently on many different devices. Figure 7, for example, shows EfficientNet-B0 can be compressed into networks that are 10% faster than MNasNet on the Samsung S20 GPU.

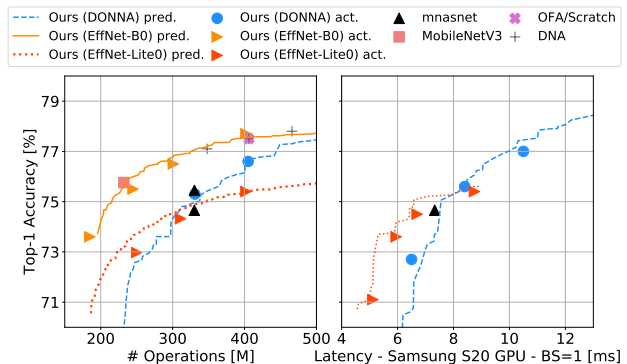


Figure 7: Compressing EfficientNet-B0, targeting # operations (left), and latency on a Samsung S20 GPU (right).

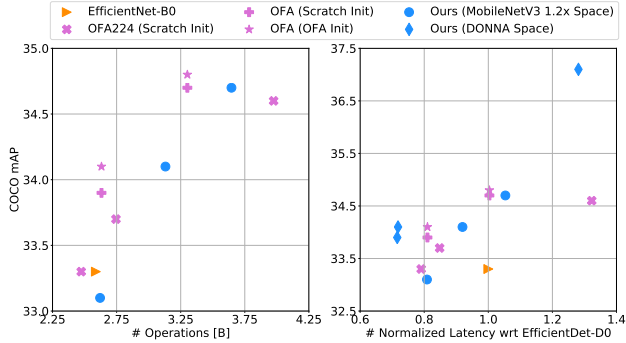


Figure 8: Object detection performance of DONNA backbones. Models transferred using DONNA are on par or better than OFA-224 models for both operations and latency, also when looking at the block-level granular MobileNetV3 (1.2 \times) search space that is used on the layer-level in OFA-224. In the DONNA search space, our solution has up to 2.4% higher mAP at the same latency as the OFA models.

In the DONNA compression pipeline, the EfficientNet search space splits EfficientNet-B0 into 5 blocks and uses it as the reference model. Every replacement block $B_{n,m}$ considered in compression is smaller than the corresponding reference block. 1135 epochs of training are spent in total to build an accuracy predictor: 135 blocks are trained using BKD, and 20 architectures are trained for 50 epochs as prediction targets. This is roughly equivalent to the resources needed for training 3 networks from scratch. Figure 7 shows DONNA finds a set of smaller, Pareto optimal versions of EfficientNet-B0 both in the number of operations and on-device. These are on-par with MobileNetV3 [11] in the number of operations and 10% faster than MnasNet [28] on device. For Samsung S20, the accuracy predictor is calibrated, as these models have no SE and Swish in the head and stem as in the EfficientNet-B0 reference.

4.2. Object Detection on MS-COCO

The DONNA architectures transfer to other tasks such as object detection on MS COCO [17]. To this end, we use the EfficientDet-D0 [30] detection architecture, replacing its EfficientNet-B0 [29] backbone with backbones originally designed for ImageNet classification with DONNA. For training, we use the hyperparameters given in [32] with the minor modification of increasing the total batch size to 128. For the EfficientDet-D0 baseline, the backbone weights are initialized with weights coming from [33].

We apply DONNA to two search spaces with different objectives. Our first space is the MobileNetV3 (1.2 \times) space where we search for the models with highest predicted ImageNet accuracy at a given number of operations. In the second search, we use the DONNA space and optimize predicted ImageNet accuracy against latency on a simulator

targeting tensor compute units. In both cases, the input resolution is fixed to 224×224 . All DONNA backbones are initialized using the weights obtained from the finetuning process described in Section 3.

For OFA [3], we consider two sets of models. The first set consists of models optimized for the number of operations (FLOP) with varying input resolution coming directly from the OFA repository [2]. The second set of models, which we identify by ‘OFA-224’, are obtained by us with the same tools [2], but with the input resolution fixed to 224×224 . This makes the OFA-224 search space the same as ours up to the layerwise-vs-blockwise distinction. In the first experiment, we initialize the OFA backbone with weights from progressive shrinking released in [2]. In the second experiment, we initialize the OFA backbone with weights from from-scratch training on ImageNet using hyperparameters from [33]. After such initialization, the networks are transferred to object detection for comparison with each other and with models obtained by DONNA. The comparison of the two experiments shows the benefit of OFA-style training is limited when the weights are transferred to a downstream task. (See Figure 8.) The gap between OFA-style training and training from scratch, which is up to 1.4% top-1 on ImageNet, decreases to 0.2% mAP on COCO, reducing its importance. We discuss this point further in Appendix B.

In comparing with DONNA models, we make two key observations in Figure 8. First, models transferred after a search using DONNA are on-par or better than OFA-224 models for both operations and latency. Second, models transferred from the DONNA space outperform OFA models up to 2.4% mAP on the validation set in latency. However, these DONNA models are not competitive for number of operations as they use grouped convolutions.

5. Conclusion

This paper proposes DONNA, a novel approach for rapid scenario-aware NAS in diverse search spaces. Through the use of a model accuracy predictor, built through knowledge distillation, DONNA finds state-of-the-art networks for a variety of deployment scenarios: in terms of number of parameters and operations, and in terms of latency on Samsung S20 and the Nvidia V100 GPU. In ImageNet classification, architectures found by DONNA are 20% faster than EfficientNet-B0 and MobileNetV2 on V100 at similar accuracy and 10% faster with 0.5% higher accuracy than MobileNetV2-1.4x on a Samsung S20 smartphone. In object detection, DONNA finds networks with up to 2.4% higher mAP at the same latency compared to OFA. Interestingly, the DONNA accuracy predictor generalizes to unseen architectures. This enables the pipeline to be used for quick search-space extensions (e.g. adding ShiftNets) and exploration, as well as for on-device network compression.

References

- [1] J. Blank and K. Deb. Pymoo: Multi-objective optimization in python. *IEEE Access*, 8:89497–89509, 2020. [5](#), [6](#)
- [2] Han Cai, Chuang Gan, Tianzhe Wang, Zhekai Zhang, and Song Han. once-for-all. <https://github.com/mit-han-lab/once-for-all>, 2020. [5](#), [6](#), [8](#), [11](#), [13](#)
- [3] Han Cai, Chuang Gan, Tianzhe Wang, Zhekai Zhang, and Song Han. Once-for-all: Train one network and specialize it for efficient deployment. *Int. Conf. Learn. Represent.*, 2020. [1](#), [2](#), [3](#), [5](#), [6](#), [7](#), [8](#), [13](#)
- [4] Han Cai, Ligeng Zhu, and Song Han. ProxylessNAS: Direct neural architecture search on target task and hardware. *Int. Conf. Learn. Represent.*, 2019. [2](#), [3](#), [11](#)
- [5] Xin Chen, Lingxi Xie, Jun Wu, and Qi Tian. Progressive DARTS: Bridging the optimization gap for nas in the wild. *Int. Conf. Comput. Vis.*, 2019. [2](#)
- [6] Ekin D. Cubuk, Barret Zoph, Jonathon Shlens, and Quoc V. Le. RandAugment: Practical automated data augmentation with a reduced search space. *IEEE Conf. Comput. Vis. Pattern Recog. Worksh.*, 2020. [11](#)
- [7] Kalyanmoy Deb, Amrit Pratap, Sameer Agarwal, and TAMT Meyarivan. A fast and elitist multiobjective genetic algorithm: Nsga-ii. *IEEE transactions on evolutionary computation*, 6(2):182–197, 2002. [5](#), [6](#)
- [8] Jia Deng, Wei Dong, Richard Socher, Li-Jia Li, Kai Li, and Li Fei-Fei. Imagenet: A large-scale hierarchical image database. *IEEE Conf. Comput. Vis. Pattern Recog.*, 2009. [2](#), [4](#), [5](#), [13](#)
- [9] Thomas Elsken, Jan Hendrik Metzen, and Frank Hutter. Neural architecture search: A survey. *Journal of Machine Learning Research*, 20:1–21, 2019. [3](#)
- [10] K. Goetschalckx and M. Verhelst. Breaking high-resolution cnn bandwidth barriers with enhanced depth-first execution. *IEEE Journal on Emerging and Selected Topics in Circuits and Systems*, 9(2):323–331, 2019. [3](#)
- [11] Andrew Howard, Mark Sandler, Grace Chu, Liang-Chieh Chen, Bo Chen, Mingxing Tan, Weijun Wang, Yukun Zhu, Ruoming Pang, Vijay Vasudevan, Quoc V. Le, and Hartwig Adam. Searching for mobilenetv3. *Int. Conf. Comput. Vis.*, 2019. [1](#), [3](#), [5](#), [7](#), [8](#), [13](#)
- [12] Jie Hu, Li Shen, Samuel Albanie, Gang Sun, and Enhua Wu. Squeeze-and-excitation networks. *IEEE Conf. Comput. Vis. Pattern Recog.*, 2018. [5](#), [7](#), [14](#)
- [13] Gao Huang, Yu Sun, Zhuang Liu, Daniel Sedra, and Kilian Weinberger. Deep networks with stochastic depth. *Eur. Conf. Comput. Vis.*, 2016. [11](#)
- [14] Maurice G Kendall. A new measure of rank correlation. *Biometrika*, 30(1/2):81–93, 1938. [4](#), [12](#)
- [15] Diederik P Kingma and Jimmy Ba. Adam: A method for stochastic optimization. *arXiv preprint arXiv:1412.6980*, 2014. [11](#)
- [16] Changlin Li, Jiefeng Peng, Liuchun Yuan, Guangrun Wang, Xiaodan Liang, Liang Lin, and Xiaojun Chang. Blockwisely supervised neural architecture search with knowledge distillation. *IEEE Conf. Comput. Vis. Pattern Recog.*, 2020. [2](#), [3](#), [4](#), [5](#), [6](#), [11](#), [12](#)
- [17] Tsung-Yi Lin, Michael Maire, Serge Belongie, Lubomir Bourdev, Ross Girshick, James Hays, Pietro Perona, Deva Ramanan, C. Lawrence Zitnick, and Piotr Dollár. Microsoft COCO: Common objects in context. *Eur. Conf. Comput. Vis.*, 2014. [2](#), [5](#), [8](#)
- [18] Hanxiao Liu, Karen Simonyan, and Yiming Yang. DARTS: Differentiable architecture search. *Int. Conf. Learn. Represent.*, 2019. [1](#), [2](#)
- [19] Ilya Loshchilov and Frank Hutter. SGDR: Stochastic gradient descent with warm restarts. *Int. Conf. Learn. Represent.*, 2017. [11](#)
- [20] Zhichao Lu, Gautam Sreeksumar, Erik Goodman, Wolfgang Banzhaf, Kalyanmoy Deb, and Vishnu Naresh Boddeti. Neural architecture transfer. May 2020. [1](#)
- [21] Jieru Mei, Yingwei Li, Xiaochen Lian, Xiaojie Jin, Linjie Yang, Alan Yuille, and Jianchao Yang. AtomNAS: Fine-grained end-to-end neural architecture search. *Int. Conf. Learn. Represent.*, 2020. [2](#)
- [22] Markus Nagel, Rana Ali Amjad, Marinus van Baalen, Christos Louizos, and Tijmen Blankevoort. Up or down? adaptive rounding for post-training quantization. In *Proceedings of Machine Learning and Systems 2020*, pages 7696–7705. 2020. [4](#)
- [23] Hieu Pham, Melody Guan, Barret Zoph, Quoc Le, and Jeff Dean. Efficient neural architecture search via parameters sharing. *Int. Conf. Machine Learning*, 2018. [2](#)
- [24] Ilija Radosavovic, Raj Prateek Kosaraju, Ross Girshick, Kaiming He, and Piotr Dollár. Designing network design spaces. In *Proceedings of the IEEE/CVF Conference on Computer Vision and Pattern Recognition*, pages 10428–10436, 2020. [7](#)
- [25] Esteban Real, Sherry Moore, Andrew Selle, Saurabh Saxena, Yutaka Leon Suematsu, Jie Tan, Quoc V. Le, and Alexey Kurakin. Large-scale evolution of image classifiers. In *Proceedings of the 34th International Conference on Machine Learning - Volume 70, ICML'17*, page 2902–2911. JMLR.org, 2017. [2](#)
- [26] Nitish Srivastava, Geoffrey Hinton, Alex Krizhevsky, Ilya Sutskever, and Ruslan Salakhutdinov. Dropout: A simple way to prevent neural networks from overfitting. *Journal of Machine Learning Research*, 15(56):1929–1958, 2014. [11](#)
- [27] Dimitrios Stamoulis, Ruizhou Ding, Di Wang, Dimitrios Lymberopoulos, Bodhi Priyantha, Jie Liu, and Diana Marculescu. Single-Path NAS: Designing hardware-efficient convnets in less than 4 hours. *ECML PKDD*, 2019. [1](#), [2](#)
- [28] Mingxing Tan, Bo Chen, Ruoming Pang, Vijay Vasudevan, Mark Sandler, Andrew Howard, and Quoc V. Le. MnasNet: Platform-aware neural architecture search for mobile. *IEEE Conf. Comput. Vis. Pattern Recog.*, 2019. [1](#), [2](#), [6](#), [7](#), [8](#), [11](#)
- [29] Mingxing Tan and Quoc V. Le. Efficientnet: Rethinking model scaling for convolutional neural networks. *Int. Conf. Machine Learning*, 2019. [1](#), [3](#), [8](#), [11](#)
- [30] Mingxing Tan, Ruoming Pang, and Quoc V. Le. Efficientdet: Scalable and efficient object detection. *IEEE Conf. Comput. Vis. Pattern Recog.*, 2020. [5](#), [8](#)
- [31] Alvin Wan, Xiaoliang Dai, Peizhao Zhang, Zijian He, Yuan-dong Tian, Saining Xie, Bichen Wu, Matthew Yu, Tao Xu,

- Kan Chen, Peter Vajda, and Joseph E. Gonzalez. FB-NetV2: Differentiable neural architecture search for spatial and channel dimensions. *IEEE Conf. Comput. Vis. Pattern Recog.*, 2020. 2
- [32] Ross Wightman. efficientdet-pytorch. <https://github.com/rwightman/efficientdet-pytorch>, 2020. 8
- [33] Ross Wightman. pytorch-image-models. <https://github.com/rwightman/pytorch-image-models>, 2020. 5, 7, 8, 11
- [34] Bichen Wu, Xiaoliang Dai, Peizhao Zhang, Yanghan Wang, Fei Sun, Yiming Wu, Yuandong Tian, Peter Vajda, Yangqing Jia, and Kurt Keutzer. FBNet: Hardware-aware efficient convnet design via differentiable neural architecture search. *IEEE Conf. Comput. Vis. Pattern Recog.*, 2019. 2
- [35] Bichen Wu, Alvin Wan, Xiangyu Yue, Peter Jin, Sicheng Zhao, Noah Golmant, Amir Gholaminejad, Joseph Gonzalez, and Kurt Keutzer. Shift: A zero flop, zero parameter alternative to spatial convolutions. In *Proceedings of the IEEE Conference on Computer Vision and Pattern Recognition (CVPR)*, June 2018. 7
- [36] Yuhui Xu, Lingxi Xie, Xiaopeng Zhang, Xin Chen, Guojun Qi, Qi Tian, and Hongkai Xiong. PC-DARTS: Partial channel connections for memory-efficient architecture search. *Int. Conf. Learn. Represent.*, 2020. 2
- [37] Jiahui Yu, Pengchong Jin, Hanxiao Liu, Gabriel Bender, Pieter-Jan Kindermans, Mingxing Tan, Thomas Huang, Xiaodan Song, Ruoming Pang, and Quoc Le. BigNAS: Scaling up neural architecture search with big single-stage models. *Eur. Conf. Comput. Vis.*, 2020. 1
- [38] Barret Zoph and Quoc V. Le. Neural architecture search with reinforcement learning. *Int. Conf. Learn. Represent.*, 2017. 2
- [39] Barret Zoph, Vijay Vasudevan, Jonathon Shlens, and Quoc V. Le. Learning transferable architectures for scalable image recognition. *IEEE Conf. Comput. Vis. Pattern Recog.*, 2018. 2

Appendix

A. Experimental Details

A.1. Hyperparameters for training and distillation

All reference models for each search space are **trained from scratch** for 450 epochs on 8 GPUs up to state-of-the-art accuracy using the hyperparameters given in [33] for EfficientNet-B0 [29]. More specifically, we use a total batch size of 1536 with an initial learning rate of 0.096, RMSprop with momentum of 0.9, RandAugment data augmentation [6], exponential weight-averaging, dropout [26] and stochastic depth [13] of 0.2, together with a learning rate decay of 0.97 every 2.4 epochs.

Blockwise knowledge distillation (BKD) is done by training every block for a single epoch. During this epoch, we apply a cosine learning rate schedule [19] considering 20 steps, an initial learning rate of 0.01, a batch size of 256, the Adam [15] optimizer, and random cropping and flipping as data augmentation.

Finetuning is done via end-to-end knowledge distillation (EKD) by using hard ground truth labels and the soft labels of the reference model, see Figure 3(b). We use the same hyperparameters used for training from scratch with the following changes: a decay of 0.9 every 2 epochs, the initial learning rate divided by 5 and no dropout, stochastic depth nor RandAugment. Depending on the reference model and the complexity of the search space, finetuning achieves full from-scratch accuracy in 15-50 epochs, see Figure 9.

A.2. Hardware measurements

All complexity measurements used throughout the text, either hardware-aware or hardware-agnostic, are gathered as follows:

- **Nvidia V100 GPU** latency measurements are done in Pytorch 1.4 with CUDNN 10.0. In a single loop, 20 batches are sent to GPU and executed, while the GPU is synced before and after every iteration. The first 10 batches are treated as a warm-up and ignored; the last 10 are used for measurements. We report the fastest measurement as the latency.
- Measurements on the **Samsung S20 GPU** are always done with a batch-size of 1, in a loop running 30 inferences, after which the system cools down for 1 minute. The average latency is reported.
- The **number of operations** and **number of parameters** are measured using the ptflops framework (<https://pypi.org/project/ptflops/>).

Table 3: Specific references for where the model accuracy numbers reported in the manuscript are taken from.

| Baseline Model | ImageNet Top-1 Val | Reference |
|---------------------|--------------------|-----------------|
| EfficientNet-B0 | 77.7 | Ours, with [33] |
| SPNASNet-100 | 74.084 | From [33] |
| MNASNet-B1-1.0x | 74.658 | From [33] |
| MNASNet-A1-1.0x | 75.448 | From [33] |
| MNASNet-A1-1.4x | 77.2 | From [28] |
| FBNet-C-100 | 78.124 | From [33] |
| MobileNetV2 (1.0x) | 72.970 | From [33] |
| MobileNetV2 (1.4x) | 76.516 | From [33] |
| MobileNetV3 (Large) | 75.766 | From [33] |
| ProxyLessNas CPU | 75.3 | From [4] |
| ProxyLessNas GPU | 75.1 | From [4] |
| ProxyLessNas Mobile | 74.6 | From [4] |
| ResNet34 | 73.3 | TorchVision |
| ResNet50 | 76.15 | TorchVision |
| OFA389 | 77.5 | Ours, with [33] |
| DNA-A | 77.1 | From [16] |
| DNA-B | 77.5 | From [16] |
| DNA-C | 77.8 | From [16] |
| DNA-D | 78.4 | From [16] |

- Latency measurement on the **simulator** targeting tensor compute units is done with a batch-size of 1. We report the fastest measurement as latency.

All complexity metrics for the reference models shown throughout the text are measured using this same setup.

A.3. Accuracy of baseline models

Accuracy is taken to be the highest reported in [33], the highest reported in the paper, or trained from scratch using the EfficientNet-B0 hyperparameters used in the [33] repository, see Table 3. This is the case for EfficientNet-B0 (our training), MobileNetV2, MNASNet, SPNASNet and FBNet. OFA/Scratch is the “flops@389M_top1@79.1_finetime@75” model from [2] trained from scratch using the hyperparameters used for EfficientNet-B0 in [33]. Note that these baselines are competitive. MobileNetV2 for example, typically has an accuracy of around 72%, while the training in [33] pushes that to 73%. ProxylessNas [4] and DNA [16] accuracies are taken from their respective papers. ResNet accuracy is used from Torchvision, but can probably be improved.

A.4. Comments on Accuracy Predictors

A.4.1 Size of the Architecture Library

Tables 4 and 5 show the impact of the size of the Architecture Library used to fit the linear predictor. The tables show

Table 4: Ranking quality for MobileNetV3 (1.2×) using DONNA, as function of the size of the Architecture Library. ‘X’T indicates that ‘X’ targets were used to fit the predictor.

| Metric | DNA [16] | 10T | 20T | 30T | 40T |
|------------------|----------|------|------|------|------|
| Kendall-Tau [14] | 0.74 | 0.79 | 0.79 | 0.8 | 0.82 |
| MSE [top-1%] | NA | 0.07 | 0.09 | 0.09 | 0.08 |

Table 5: Ranking quality for DONNA, as a function of the size of the Architecture Library. ‘X’T indicates that ‘X’ targets were used to fit the predictor.

| Metric | DNA [16] | 10T | 20T | 30T | 40T |
|------------------|----------|------|------|-----|------|
| Kendall-Tau [14] | 0.77 | 0.87 | 0.87 | 0.9 | 0.9 |
| MSE [top-1%] | NA | 0.28 | 0.18 | 0.2 | 0.19 |

how performance varies on a test set of finetuned models for the MobileNetV3 (1.2×) and DONNA search spaces, respectively. Note how the ranking quality, as measured by Kendall-Tau (KT) [14], is always better in this work than in DNA [16]. On top of that, DNA [16] only ranks models within the search space and does not predict accuracy itself. Another metric to estimate the accuracy predictor’s quality is the Mean-Squared-Error (MSE) in terms of predicted top-1 accuracy on the ImageNet validation set. Note that for the MobileNetV3 (1.2×) search space, 20 target accuracies are sufficient for a good predictor, as shown in Table 4. We use the same amount of targets for the EfficientNet-B0, MobileNetV3 (1.0×) and ProxylessNas (1.3×) search spaces. For the DONNA search space, we use 30 target accuracies, see Table 5. Note that the linear accuracy predictor can improve overtime, whenever the Architecture Library is expanded. As predicted Pareto-optimal architectures are finetuned to full accuracy, those results can be added to the library and the predictor can be fitted again using this extra data.

A.4.2 Choice of Quality Metrics

Apart from using the Noise-To-Signal-Power-Ratio (NSR) (See Section 3), other quality metrics can be extracted and used in an accuracy predictor as well. All quality metrics are extracted on a held-out validation set, sampled from the ImageNet training set, which is different from the default ImageNet validation set in order to prevent overfitting. Three other types of quality metrics are considered on top of the metric described in equation 1: one other block-level metric based on L1-loss and two network-level metrics. The block-level metric measures the normalized L1-loss between ideal feature map Y_n and the block $B_{n,m}$ ’s output feature map $\tilde{Y}_{n,m}$. It can be described as the Noise-

Table 6: Comparing different quality metrics: NSR (Equation 1), L1, network-level loss and top-1 accuracy for DONNA.

| Ranking Metric | DNA [16] | NSR | L1 | Loss | Top-1 |
|------------------|----------|------|------|------|-------|
| Kendall-Tau [14] | 0.77 | 0.9 | 0.89 | 0.89 | 0.88 |
| MSE [top-1%] | NA | 0.19 | 0.23 | 0.41 | 0.44 |

Table 7: Comparing the quality of accuracy predictors for different search spaces. Predicted accuracy is the top-1 validation accuracy on ImageNet.

| Search-Space | Kendall Tau[14] | MSE [top-1%] |
|---------------------|-----------------|--------------|
| DONNA | 0.9 | 0.19 |
| EfficientNet-B0 | 0.91 | 0.15 |
| MobileNetV3 (1.0×) | 0.97 | 0.13 |
| MobileNetV3 (1.2×) | 0.82 | 0.08 |
| ProxyLessNas (1.3×) | 0.95 | 0.04 |

to-Signal-Amplitude ratio:

$$\mathcal{L}(W_{n,m}; Y_{n-1}, Y_n) = \frac{1}{C} \sum_{c=0}^C \frac{\|Y_{n,c} - \tilde{Y}_{n,m,c}\|_1}{\sigma_{n,c}} \quad (3)$$

The two network-level metrics are the loss and top-1 accuracy extracted on the separate validation set. The network-level metrics are derived by replacing only block B_n in the reference model with the block-under-test $B_{n,m}$ and then validating the performance of the resulting network. Table 6 compares the performance of the 4 different accuracy predictors built on these different styles of features. Although they are conceptually different, they all lead to a very similar performance on the test set with NSR outperforming the others slightly. Because of this, the NSR metric from equation 1 is used throughout the text.

A.4.3 Accuracy predictors for different search-spaces

Similar to the procedures discussed in section 3, accuracy models are built for different reference architectures in different search spaces: EfficientNet-B0, MobileNetV3 (1.0×), MobileNetV3 (1.2×) and ProxylessNas (1.3×). The performance of these models is illustrated in Table 7. Note that we can generate reliable accuracy predictors for all of these search spaces, with very high Kendall-Tau ranking metrics and low MSE on the prediction. The Kendall-Tau value on the MobileNetV3 (1.2×) search space is lower than the others, as the test set is larger for this space than for the others. The model is still reliable, as is made apparent by the very low MSE metric.

A.5. Finetuning speed

Depending on the search space’s complexity, the used reference model in BKD, and the teacher in end-to-end

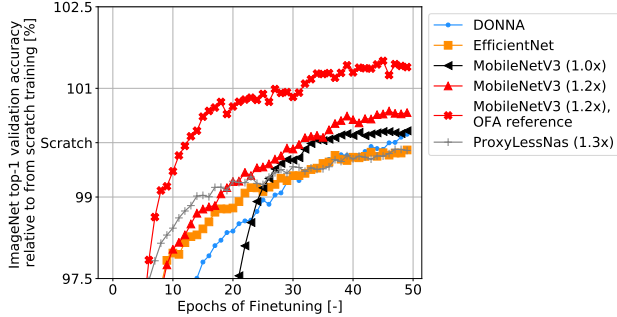


Figure 9: Speed at which BKD-initialized subsampled models can be finetuned for different search spaces. Models in DONNA, EfficientNet and ProxyLessNas (1.3 \times) converge to the accuracy of 450-epoch from scratch training in less than 50 epochs using the BKD initialization point, a $9\times$ speedup. Models in the MobileNetV3 search space converge in about 30 epochs, a $15\times$ speedup. If the supernet from OFA [2, 3] is used as a reference model and teacher model in the DONNAPipeline for MobileNetV3 (1.2 \times), from-scratch 450 epoch accuracy is even achieved in less than 15 epochs, a $30\times$ speed up.

knowledge distillation (EKD), finetuning can be faster or slower in terms of epochs. We always calibrate the finetuning process to be on-par with training from scratch for a fair comparison, but networks can be trained longer for even better results. With the hyperparameters for EKD given in Appendix A.1, Figure 9 shows that finetuning rapidly converges to from-scratch training accuracy for a set of subsampled models in different search spaces. The fastest convergence takes only 15 epochs, while 50 epochs are more typical for most of the examples. Finetuning speed also depends on the final accuracy of the sub-sampled model. With an accuracy very close to the accuracy of the reference model, larger models typically converge slower using EKD than smaller models with a lower accuracy. For the smaller models, the teacher’s guidance dominates more, which leads to faster finetuning.

A.6. Models for various search-spaces

Figure 10 illustrates predicted and measured performance of DONNA models in terms of number of parameters, number of operations, on an Nvidia V100 GPU and a Samsung S20 GPU, as in the main text. On top of this, predicted Pareto curves for a variety of other search-spaces are shown: MobileNetV3 (1.0 \times), MobileNetV3 (1.2 \times) and ProxyLessNas (1.3 \times). For these other search-spaces, we perform predictor-based searches in each of the scenarios, illustrating their respective predicted Pareto-optimal trendlines. The quality of these predictors is given in Table 7. For the extra search spaces, some optimal models have

been finetuned for specific scenarios to verify the predicted curve’s validity. We do not verify all search spaces in all scenarios to save on our compute resources, but every search space is confirmed in at least one scenario. For every search space, the same accuracy predictor is used across all scenarios. We argue that if the predicted curve can be confirmed in one scenario, it is likely accurate for the other scenarios.

MobileNetV3 (1.0 \times) and MobileNetV3 (1.2 \times) are confirmed in terms of number of operations in Figure 10 (mid-left). ProxyLessNas (1.3 \times) is confirmed on an Nvidia V100 GPU in Figure 10 (mid-right). In the MobileNetV3 (1.0 \times) space, we find networks that are on-par with the performance of MobileNetV3 [11] in terms of accuracy for the same number of operations, which validates that DONNA can find the same optimized networks as other methods in the same or similar search spaces. Note that the DONNA outperforms all other search spaces on hardware platforms and in terms of number of parameters, which motivates our choice to introduce the new design space. The DONNA space is only outperformed in terms of Pareto-optimality when optimizing for the number of operations, a proxy metric.

B. Model Transfer Study

In this section, we further investigate the transfer properties of DONNA backbones in an object detection task. Our data hints towards two conclusions: (1) ImageNet top-1 validation is a good predictor for COCO mAP if models are sampled from a similar search space and if they are trained using the same hyperparameters and starting from the same initialization and (2) higher accuracies on ImageNet achieved through progressive shrinking in OFA do not transfer to significantly higher COCO mAP. The models under study are the same set as in Section 4.2.

These conclusions are apparent from Figure 11. Here, we plot the COCO Val mAPs of the detection architectures against the ImageNet Val top-1 accuracies of their respective backbones. First, we see that OFA models trained from scratch (OFA Scratch and OFA224) and models found in the similar MobileNetV3 (1.2 \times) search space through DONNA, transfer very similarly to COCO. Models found in the DONNA search space reach higher COCO mAP than expected based on their ImageNet top-1 accuracy. We suspect that such bias occurs because instead of strictly relying on depthwise convolutions, which is the case for MobileNetV3 (1.2 \times) space, grouped convolutions are used in the DONNA search space. Second, we find that while OFA models with OFA training obtain around 1.0-1.5 percent higher accuracy on ImageNet [8] than the same models trained from scratch, this increased accuracy does not transfer to a meaningful gain in downstream tasks such as object detection. This phenomenon is illustrated in Fig-

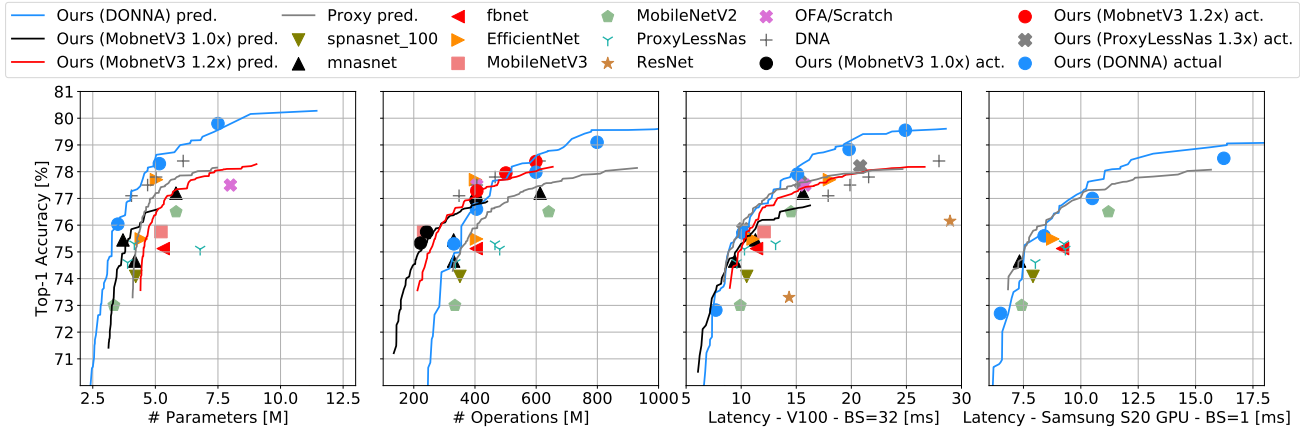


Figure 10: Trendlines and models found by DONNA optimizing for the number of parameters (left), the number of operations (mid left), inference time on an Nvidia V100 GPU (mid right) and a commercially available Samsung S20 smartphone GPU (right). Best viewed in color.

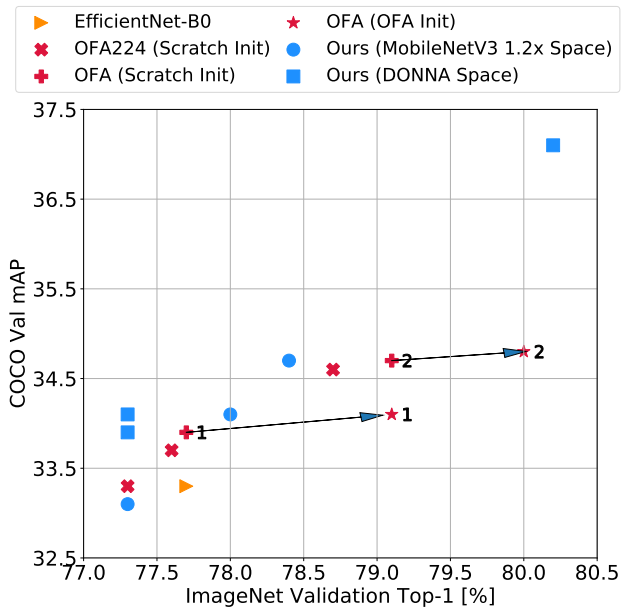


Figure 11: Transfer performance of DONNA backbones to object detection. For DONNA models, COCO validation mAP correlates well with the ImageNet Validation Top-1 accuracy. This is also the case for OFA models, if they are pretrained on ImageNet under the same or similar circumstances. If the OFA models are trained through progressive shrinking, their higher ImageNet accuracy does not transfer to a higher performance on MS-COCO.

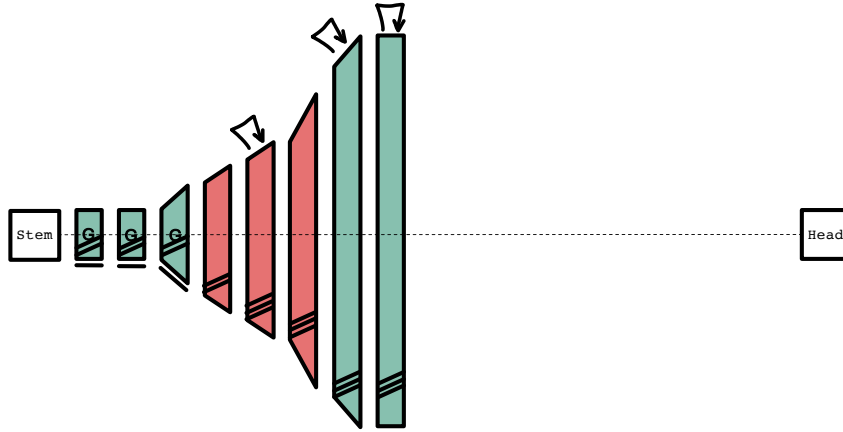
ure 11, where the same OFA models are trained on MS-COCO, either starting from weights trained on ImageNet from scratch or starting from weights obtained through progressive shrinking on ImageNet. For one of these models,

the 1.4% gain in ImageNet validation accuracy only translates into 0.1% higher mAP on COCO. This observation motivates the choice that throughout the text, we compare to OFA-models which are trained from scratch rather than through progressive shrinking.

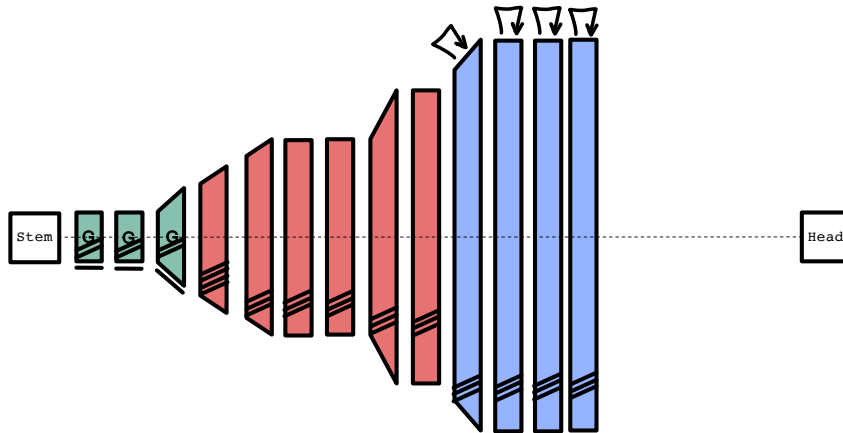
C. Model Visualizations

Figures 12, 13, 14, 15 and 16 visualize some of the diverse network architectures found through DONNA in the DONNA search space. Results are shown for a simulator, the Nvidia V100 GPU, the number of operations, the number of parameters, and the Samsung S20 GPU. Note that all of these networks have different patterns of Squeeze-and-Excite (SE [12]) and activation functions (whenever SE is used, Swish is also used), channel scaling, expansion rates, and kernel factors, as well as varying network depths. In Figure 12, grouped convolutions are also used as parts of optimal networks as a replacement of depthwise separable kernels.

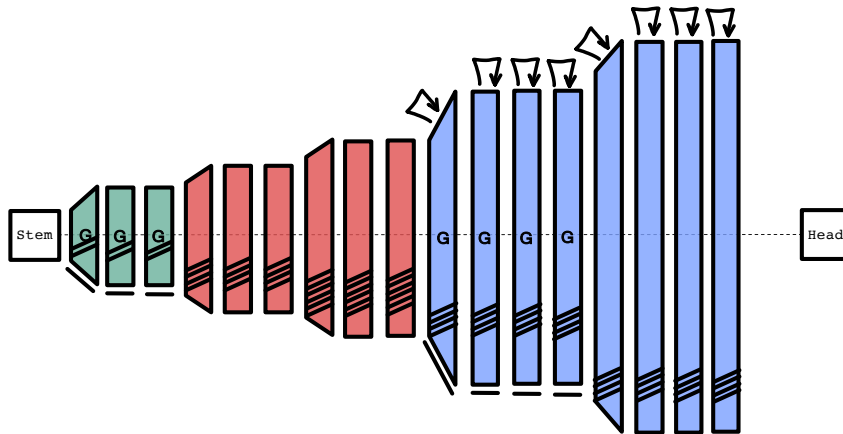
Figure 17 and 18 illustrate optimal EfficientNet-Style networks for the number of operations and the Samsung S20 respectively, as taken from Figure 7. Note how these networks are typically narrower, with higher expansion rates than the DONNA models, which makes them faster or more efficient in some cases. However, EfficientNet-Style models cannot achieve higher accuracy than 77.7% top-1 on ImageNet validation using 224×224 images, while the DONNA search space can achieve an accuracy higher than 80% in that case.



(a) DONNA for a simulator targeting tensor compute in a mobile SoC, 73.7% at $0.45\times$ the latency of EfficientNet-B0.

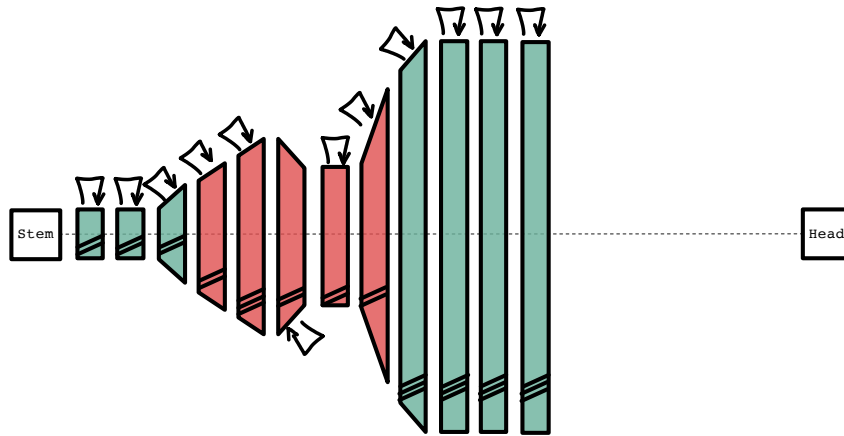


(b) DONNA for a simulator targeting tensor compute in a mobile SoC, 77.25% at $0.60\times$ the latency of EfficientNet-B0.

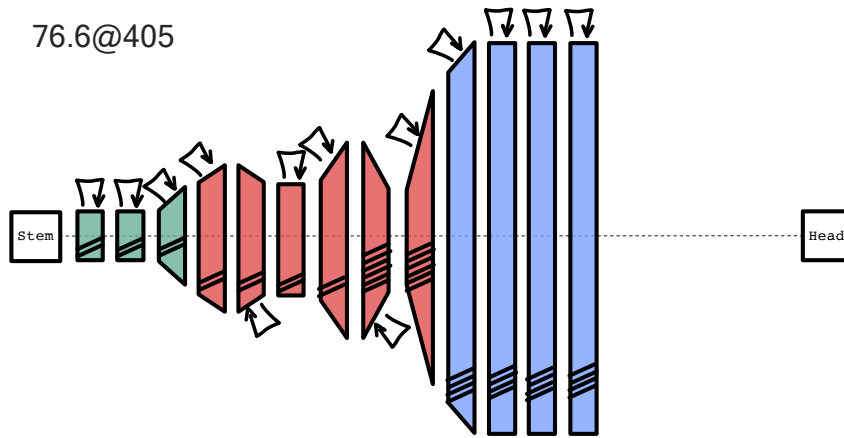


(c) DONNA for a simulator targeting tensor compute in a mobile SoC, 80.2% at $1.25\times$ the latency of EfficientNet-B0.

Figure 12: Example models found through DONNA in the DONNA search space, Pareto-optimal on ImageNet for a simulator targeting tensor compute units in a mobile SoC. The Box-color indicates kernel-size: green (3), blue (5) and red (7). Every box is an inverted residual bottleneck with depthwise-separable (plain) or grouped (line under the box) layers. The box height is related to the number of channels. The number of dashed lines per box indicate the expansion rate, the arrows on top indicate whether or not Squeeze-and-Excite and Swish is used.

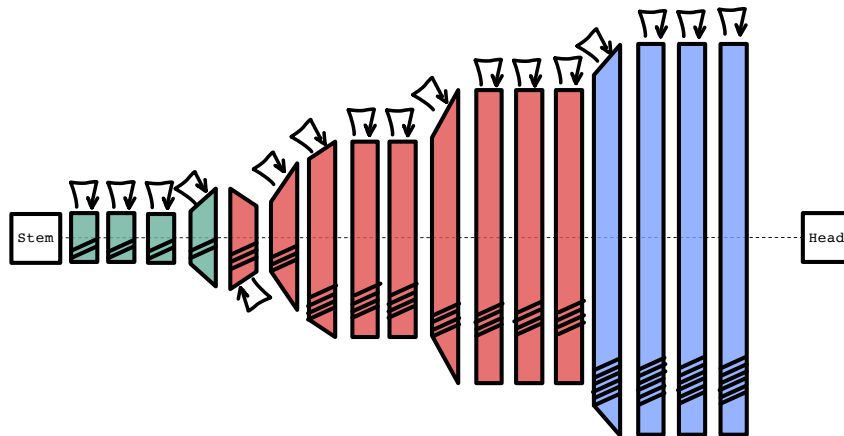


(a) DONNA for number of operations, 75.3% @ 331 MFLOP



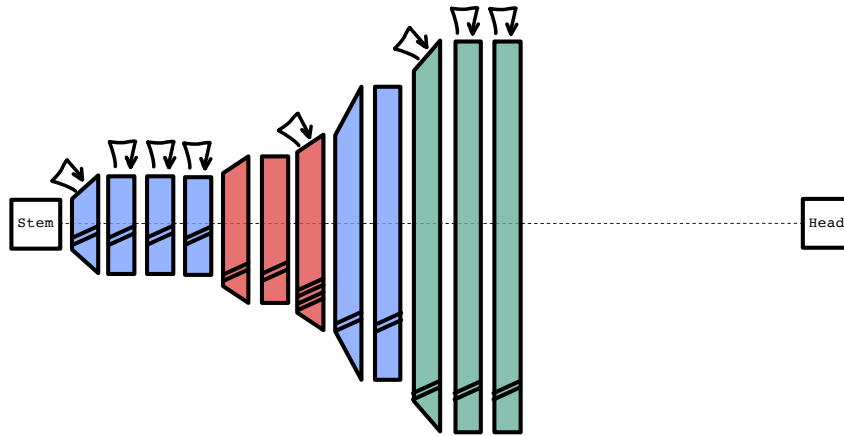
76.6@405

(b) DONNA for number of operations, 76.6% @ 405 MFLOP

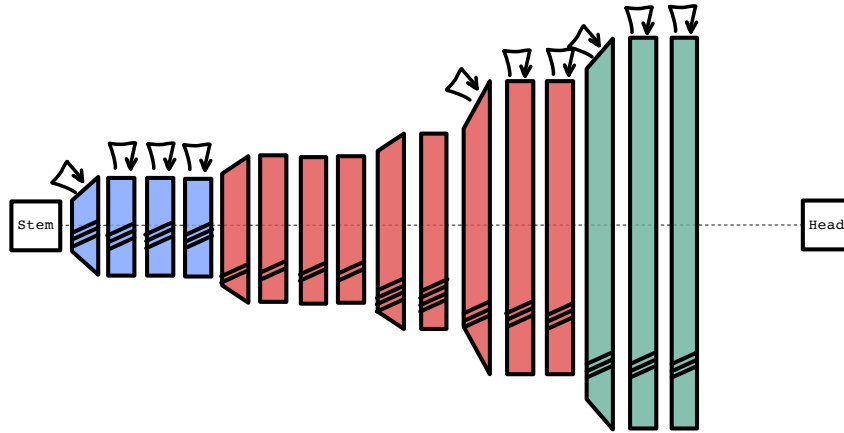


(c) DONNA for number of operations, 79.1% @ 800 MFLOP

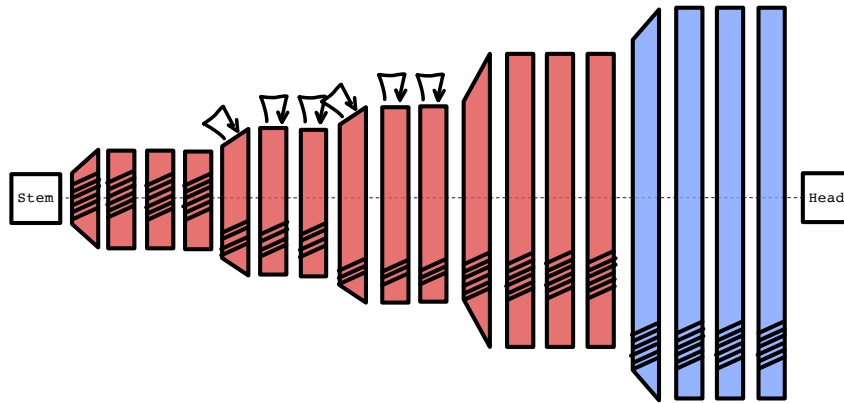
Figure 14: Example models found through DONNA in the DONNA search space, Pareto-optimal on ImageNet optimized for the number of operations. The Box-color indicates kernel-size: green (3), blue (5) and red (7). Every box is an inverted residual bottleneck with depthwise-separable (plain) or grouped (line under the box) layers. The box height is related to the number of channels. The number of dashed lines per box indicate the expansion rate, the arrows on top indicate whether or not Squeeze-and-Excite is used. Note that it is optimal to use SE in every block.



(a) DONNA for number of parameters, 76.0% @ 3.5 million parameters.

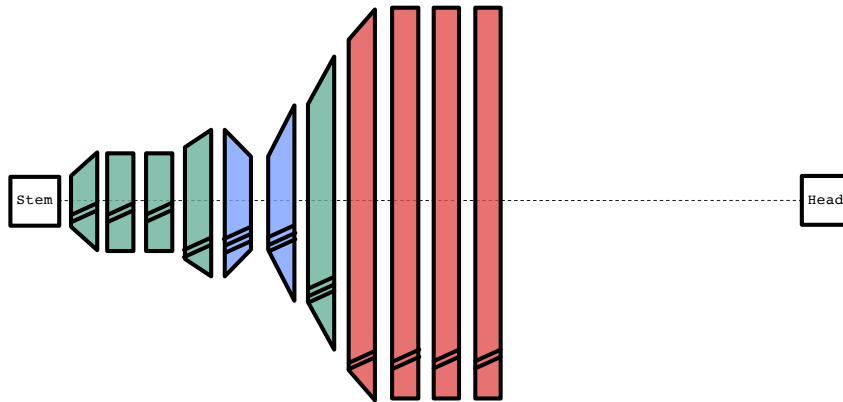


(b) DONNA for number of parameters, 78.3% @ 5.16 million parameters.

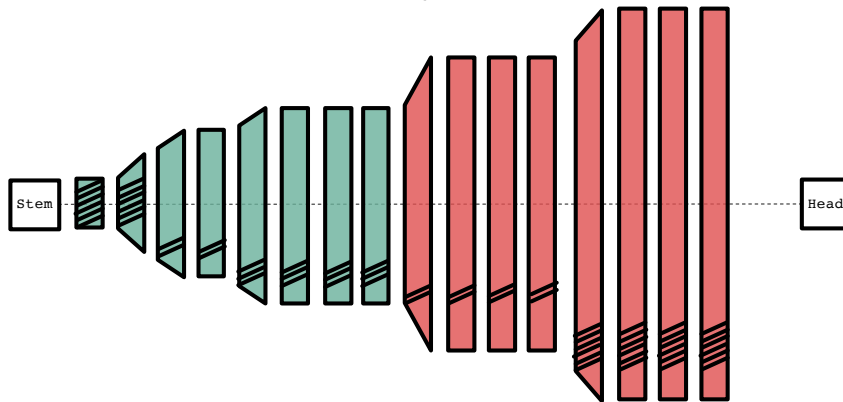


(c) DONNA for number of parameters, 80.0% @ 7.5 million parameters.

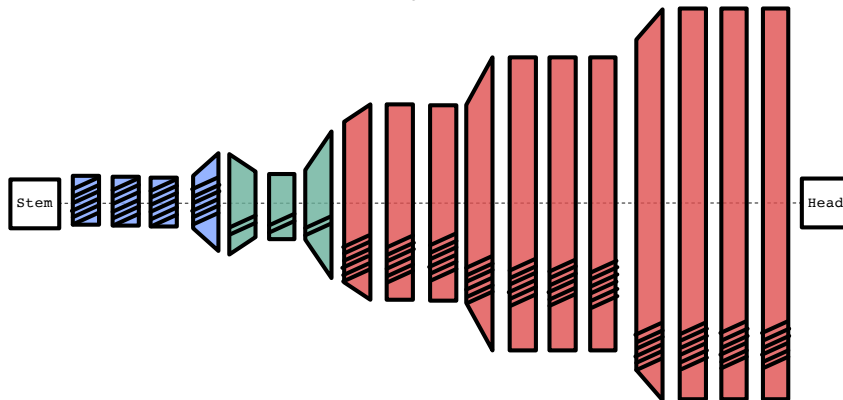
Figure 15: Example models found through DONNA in the DONNA search space, Pareto-optimal on ImageNet optimized for the number of parameters. The Box-color indicates kernel-size: green (3), blue (5) and red (7). Every box is an inverted residual bottleneck with depthwise-separable (plain) or grouped (line under the box) layers. The box height is related to the number of channels. The number of dashed lines per box indicate the expansion rate, the arrows on top indicate whether or not Squeeze-and-Excite and Swish is used.



(a) DONNA for the Samsung S20 GPU, 72.7% @ 6.5 ms.

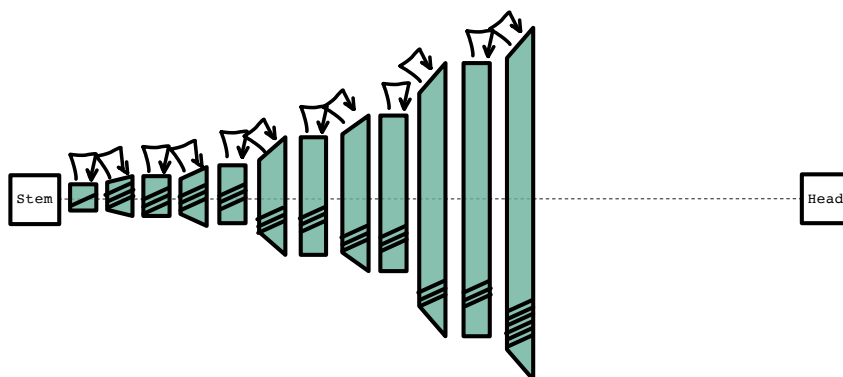


(b) DONNA for the Samsung S20 GPU, 76.96% @ 10.5 ms.

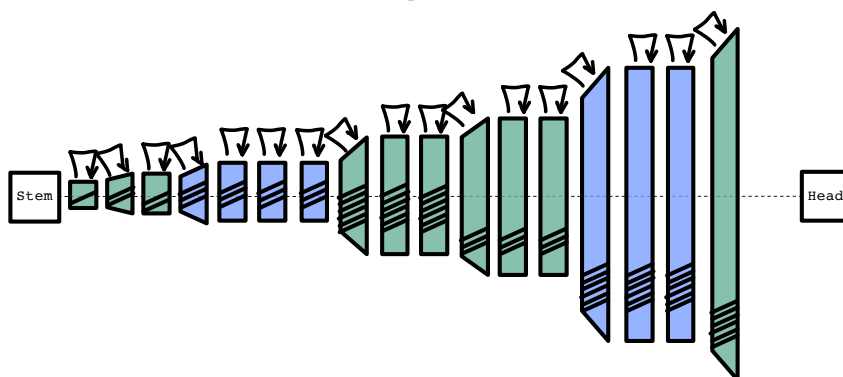


(c) DONNA for the Samsung S20 GPU, 78.9% @ 16.2 ms.

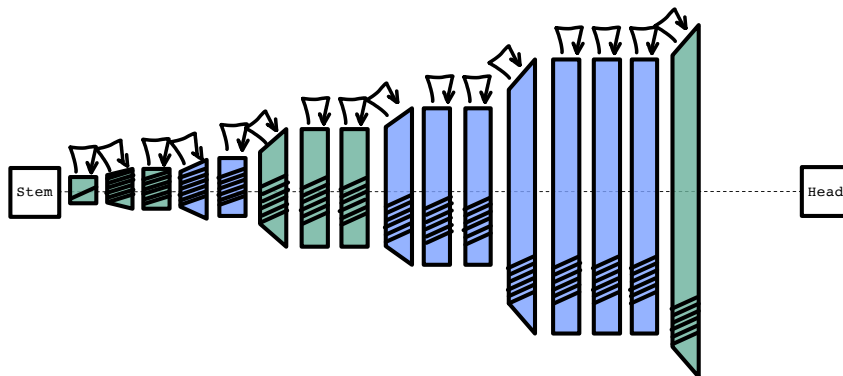
Figure 16: Example models found through DONNA in the DONNA search space, Pareto-optimal on ImageNet optimized for the Samsung S20 GPU. The Box-color indicates kernel-size: green (3), blue (5) and red (7). Every box is an inverted residual bottleneck with depthwise-separable (plain) or grouped (line under the box) layers. The box height is related to the number of channels. The number of dashed lines per box indicate the expansion rate, the arrows on top indicate whether or not Squeeze-and-Excite and Swish is used.



(a) DONNA for number of operations, 73.4% @ 185 MFLOP

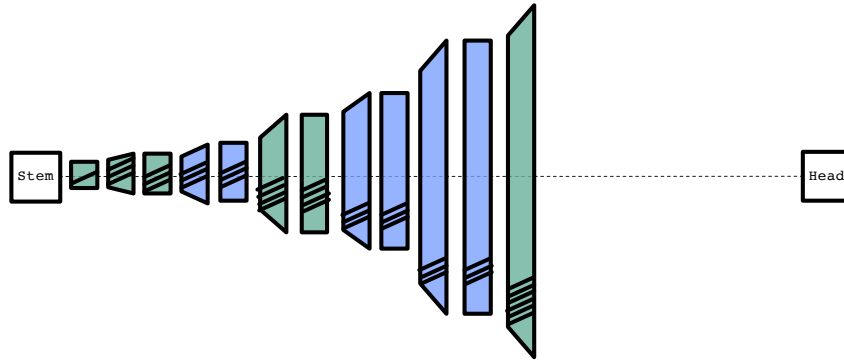


(b) DONNA for number of operations, 76.6% @ 301 MFLOP

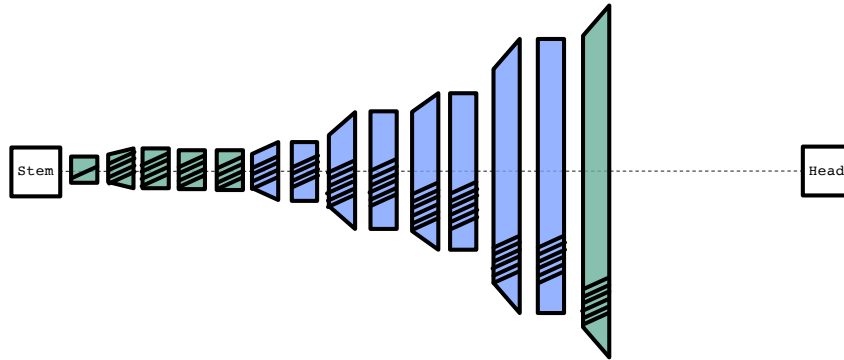


(c) DONNA for number of operations, 77.7% @ 405 MFLOP

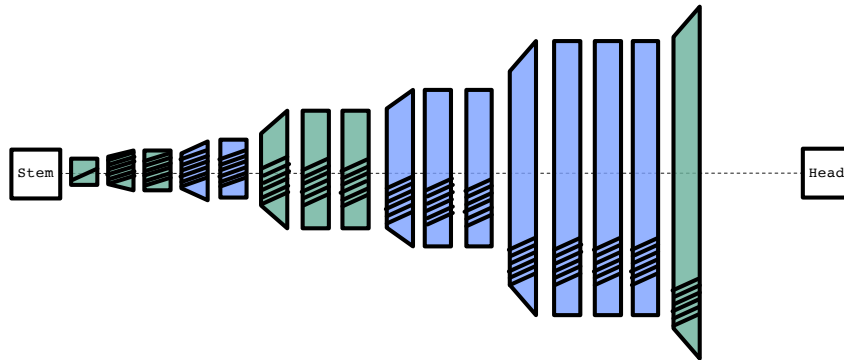
Figure 17: Example models found through DONNA in the EfficientNet-B0 search space, Pareto-optimal on ImageNet optimized for the number of operations. The Box-color indicates kernel-size: green (3), blue (5) and red (7). Every box is an inverted residual bottleneck with depthwise-separable layers. The box height is related to the number of channels. The number of dashed lines per box indicate the expansion rate, the arrows on top indicate whether or not Squeeze-and-Excite is used. Note that it is optimal to use SE in every block.



(a) DONNA for the Samsung S20 GPU, 71.5% @ 5.2 ms.



(b) DONNA for the Samsung S20 GPU, 73.6% @ 5.95 ms.



(c) DONNA for the Samsung S20 GPU, 75.4% @ 8.8 ms.

Figure 18: Example models found through DONNA in the EfficientNet search space, Pareto-optimal on ImageNet optimized for the Samsung S20 GPU. The Box-color indicates kernel-size: green (3), blue (5) and red (7). Every box is an inverted residual bottleneck with depthwise-separable layers. The box height is related to the number of channels. The number of dashed lines per box indicate the expansion rate, the arrows on top indicate whether or not Squeeze-and-Excite and Swish is used.